Article

Not peer-reviewed version

Functional Electrospun Nanofibers Loaded with Plantago Major L. Extract for Potential Use in Cutaneous Wound Healing

Javier Mauricio Anaya-Mancipe , Vanessa de Moura Queiroz , Rafael Ferreira Dos Santos , Rosane Nora Castro , Veronica da Silva Cardoso , Alane Beatriz Vermelho , Marcos Lopes Dias * , Rossana. Mara da Silva Moreira Thiré *

Posted Date: 20 February 2023

doi: 10.20944/preprints202302.0314.v1

Keywords: Electrospinning; Nanofibers; Polycaprolactone; Plantago Major L; Drug delivery; Wound dressing

Article

Functional Electrospun Nanofibers Loaded with *Plantago Major L.* Extract for Potential Use in Cutaneous Wound Healing

Javier M. Anaya-Mancipe [1,2], Vanessa M. Queiroz [1], Rafael F. dos Santos [3], Rosane N. Castro [3], Veronica S. Cardoso [4], Alane B. Vermelho [4], Marcos L. Dias [2]* and Rossana M.S.M. Thiré [1]*

[1] COPPE/Program of Metallurgical and Materials Engineering – PEMM, Universidade Federal de Rio de Janeiro – UFRJ, Rio de Janeiro RJ, Brazil; javier.anaya@metalmat.ufrj.br; queiroz.bio@gmail.com; rossana@metalmat.ufrj.br;

[2] Institute of Macromolecules Professor Eloisa Mano – IMA, Universidade Federal do Rio de Janeiro – UFRJ, Rio de Janeiro RJ, Brazil; mldiasl@ima.ufrj.br;

[3] Chemistry Institute, Graduate Program in Chemistry, Universidade Federal Rural do Rio de Janeiro – UFRRJ, Seropédica RJ, Brazil. rafael.ssantos097@hotmail.com; nora@ufrrj.br;

[4] Bioinovar – Instituto de Microbiologia Paulo de Góes, Universidade Federal do Rio de Janeiro - UFRJ, Rio de Janeiro RJ, Brazil; verocardoso@micro.ufrj.br; abvermelho@micro.ufrj.br;

* Correspondence: MLD: mldidas@ima.ufrj.br; Tel.: +55 21 98793-8585; RMSMT: rossana@metalmat.ufrj.br; Tel.: +55 21 3938-850

Abstract: *Plantago major L.* is a worldwide available plant that has been used traditionally for several medical application due to its properties such as wound healing, anti-inflammatory, antimicrobial etc. This work aimed to develop and evaluate nanostructured PCL electrospun dressing with *P. major* extract encapsulated in nanofibers for application in wound healing. The extract from leaves was obtained by extraction in a mixture of water:ethanol= 1:1 of the freeze-dried extract presented a minimum inhibitory concentration (MIC) for *Staphylococcus Aureus susceptible and* resistant to methicillin of 5.3 mg/mL, a high antioxidant capacity, but a low content of total flavonoids. Electrospun mats without defects were successfully produced using two *P. major* extract concentrations based on MIC value. The extract incorporation in PCL nanofibers was confirmed by FTIR and contact angle measurements. The PCL/*P. major* extract was evaluated by DSC and TGA demonstrating that incorporation of the extract decreases the thermal stability of the mats as well as the degree of crystallinity of PCL-based fibers. The *P. major* extract incorporation on electrospun mats produced a significant swelling degree (more than 400%) and increased the capacity of adsorbing wound exudates and moisture, important characteristics for skin healing. The extract-controlled release evaluated by in vitro study in PBS (pH, 7.4) shows that *P. major* extract delivery from the mats occurs in the first 24 h, demonstrating their potential capacity to be used in wound healing.

Keywords: electrospinning; nanofibers; polycaprolactone; *Plantago Major L*; drug delivery; wound dressing

1. Introduction

The skin is one of the body's major organs, as it plays the role of maintaining internal fluid homeostasis. It provides a barrier against environmental, chemical, mechanical, and other damages. This is why skin damage can be considered a major health problem [1-3]. Although the skin has the capacity for self-healing, wound healing can be affected and/or delayed due to infection, and necessitate the application of antibiotics [4].

Advances in regenerative medicine related to wound treatment have been studying the production of new nanostructured dressings that, in addition to serving as a protective barrier for the wound, maintain effective conditions to promote cell proliferation and migration [5,6]. Implementing intelligent and bioactive dressings, which have structures that mimic the extracellular matrix of the skin (ECM), and maintain a moist environment, while preventing bacterial colonization

in the wound bed through controlled release of drugs/antibiotics, active ingredients and/or factors that accelerate the regenerative processes, favoring the repair of damaged tissue [7-9].

In recent years it has become popular to include traditional medicine, in which drugs of natural origin are widely used, such as waxes, extracts, dyes, and essential oils, obtained from leaves, seeds, flowers, etc. combined with encapsulation methodologies such as nanoparticles, gels, nanofibers that together have shown promising results for its application in clinical practice [10-15]. One of the techniques that have been gaining prominence in this application is electrospinning, due to its wide variety of materials and solvents used that allow the production of nanostructured biomedical materials.

Electrospinning is a promising technique to create nanofibrous mats with efficient morphological and mechanical properties, allowing those materials to have a good capacity for promoting the recovery of structurally damaged tissues close to the extracellular matrix (ECM) of the skin [16,17]. These structural features have called attention to their application in regenerative medicine, which uses natural and synthetic polymers with the ability to encapsulate various active materials, drugs, and/or growth factors [18]. One of the main advantages of this process is its versatility and ease of production, producing nanostructured matrices with an ECM design that allows for rapid cell growth and adhesion. In addition, electrospinning is an easy way to functionalize the nanofibers, incorporating a wide range of bioactive additives for wound healing [19].

Polycaprolactone (PCL) is one of the most used polymers in electrospinning. It is a biodegradable polyester, highly used in the production of medical devices due to its good biocompatibility and, in addition, offers excellent characteristics for its use as an encapsulating material for the controlled release of drugs and/or active material, making it an effective polymer for biomedical applications [20,21].

Plantago major L. (*P. major*) is a perennial plant that belongs to the Plantaginaceae family. Originating from Europe, it is the most widely used species in both traditional and modern medicine [22,23]. Its use is mostly related to the implementation of the leaves in the preparation of extracts, essential oil, and pastes, among others with excellent results for the treatment of cutaneous wounds. The activity is mainly attributed to its phytochemical components such as polysaccharides, lipids, derivatives of caffeic acid, flavonoids, iridoid glycosides, and terpenoids, offering anti-inflammatory, antioxidant, analgesic, immunomodulatory, anti-ulcer and antibiotic capacities. These pharmacological properties make it a promising phytochemical for biomedical and regenerative applications [24-29].

The wound-healing capacity of the leaf extract has been proved by "in vivo" tests with animals and humans, using different pharmacology forms, such as ointment [30] and topical gel [31].

Amini and collaborators (2010) evaluated the regenerative power of the hydroalcoholic extract of *P. major L.* in burns [32]. *In vivo* tests were performed in rats varying the concentration of the extract applied at 7, 14, and 21 days. The histological analyses demonstrated a significant variation in the group of animals that received the extract with a concentration of 50 % w/v producing therapeutic action from day 21 of the study. Reina et al. (2013) evaluated *in vitro* effects in human neutrophils of *baicalein* and *aucubin* (flavonoid and glycoside, respectively) present in *P. major* leaf extract showing no cytotoxicity in LHD assays, as well as good antioxidant properties of baicalein for its use in dressings [33].

However, few works reporting studies related to the encapsulation of *Plantago major* in electrospun nanofibers were found in the literature. The search was performed using as keywords: *Plantago major*, nanofibers, and electrospinning. With these keywords, only two studies were found. The first one was performed in 2019 by Golkar et al. [34], who developed electrospun nanofibers with average diameters smaller than 250 nm using a blend of *P. major* seed mucilage (MSM) and poly(vinyl alcohol) - PVA in equal mass ratio (1:1). The authors observed a significant increase in cell proliferation when MSM was incorporated, demonstrating its ability to be implemented as a platform for cell culture and/or drug delivery.

Recently, in 2022, de Castro *et al.* [35] developed electrospun nanofibers of hyaluronic acid (HA) and PVA loaded with commercial aqueous extract from leaves of *Plantago major* for application in

 doi:10.20944/preprints202302.0314.v1

smart dressings. In this work, the authors evaluated the spinnability of the blend using maleic acid as a crosslinking agent, as well as the water adsorption capacity and interaction of the extract with the polymer blend.

Thus, the main objective of this work was to produce nanostructured bioactive polycaprolactone mats via monolithic electrospinning with the incorporation of a phyto-drug obtained from *Plantago major L.* leaves aiming potential application in skin tissue regeneration. For this, the chemical and pharmacological composition of the *P. major* extract was evaluated by HPLC. The electrospun mats were characterized morphologically by SEM and the encapsulation of the extract was evaluated by FTIR. The interaction of the extract and PCL was evaluated by DSC, TGA, and contact angle. Finally, its application as a dressing was evaluated *in vitro* considering the exudate adsorption by swelling assay and drug delivery capacity.

2. Materials and Methods

2.1. . Materials

Polycaprolactone – PCL in pellets (Mw: 70,000-90,000 g/mol; GH: 98%) was purchased from Sigma-Aldrich, São Paulo, Brazil. Dry *Plantago major L.* (*P. Major*) leaves were acquired from RioFlora (Ervas Medicinais), Rio de Janeiro, Brazil. As solvents, we used dichloromethane (DCM), *N,N*-dimethylformamide (DMF), and ethanol – PA acquired from Vetec Quimica Fina, (Rio de Janeiro Brazil). Methanol spectroscopy grade was purchased from Vetec (Rio de Janeiro, Brazil). DPPH (2,2-diphenyl-1-picryl-hydrazine), and Folin-Ciocalteau reagent were acquired from Sigma-Aldrich Chemie (Steinheim, Germany). Sodium phosphate dibasic and potassium phosphate monobasic for phosphate buffer solution (PBS) preparation were purchased from Vetec Química Fina (Rio de Janeiro, Brazil).

2.2. Plantago major L. extract preparation

The *Plantago major L.* (*P. major*) hydroalcoholic extract was prepared following the method described by Mello *et al.* (2015) with some modifications [36]. Dried *P. major* leaves (10 g) were weighed and crushed using mortar. The leaves were then placed in a flask with a hydroalcoholic solution (1:1) of ethanol/MiliQ water for 24 h at room temperature. Afterward, the suspension was put in an ultrasonic bath for 1 hour, followed by vacuum filtration and roto-evaporation at 50 °C to decrease its volume by 50%. The *P. major* extract was cooled down to room temperature, then, frozen and freeze-dried for 48 h to remove the moisture completely. Finally, the dry extract was stocked to ~4 °C.

2.3. Polymeric solutions

Three PCL solutions were prepared following methods described in previous studies adding different mass concentration of the *Plantago major* dry extract [37]. The authors used a solvent system composed by DCM/DMF (7:3) (10 wt/v% PCL). For this, 0.5 g of PCL pellets were weighed and solubilized in 3.5 mL dichloromethane, while the freeze-dried extract was suspended in 1.5 mL of DMF at two concentrations (5.3 and 10.6 wt. % relative to PCL mass) under magnetic stirring and room temperature. Subsequently, the two solutions (PCL/DCM and *P. major*/DMF) were mixed under magnetic stirring for another half hour or until a homogeneous mixture was obtained. The solutions were named as PCL_0.0, PCL_5.3, and PCL_10.6 according to the content of dry extract in relation to PCL mass.

2.4. Electrospinning process

Electrospun PCL mats with and without *Plantago major L.* extract were prepared using a horizontal electrospinning apparatus composed of Glassman High Voltage source (USA) model PS/FC 60p02.0-1, a KDS 100 series syringe pump, plastic syringe with a metallic needle, and a grounded aluminum plate collector. To facilitate samples remotion, aluminum foils were used over

 doi:10.20944/preprints202302.0314.v1

the plate collector. Five mL of each solution were transferred on a plastic syringe and metallic needle with 0.5 mm of internal diameter (22 gauds). The flow rate was kept at 0.75 mL/h, while the voltage applied was varied in the range of 15 to 20 kV, and the working distance was 12 cm. The obtained mats were named as PCL_0.0, PCL_5.3, and PCL_10.6 mats. The spinnability of the solution was evaluated by morphological analyses. To verify the effect of adding extract on the fiber diameter, an analysis of variance (ANOVA) Post hoc Test–Fisher's Least Significant difference (LSD) was performed adopting a 0.05 significance level ($p < 0.05$) [38].

2.5. Characterization

2.5.1. *In Vitro* minimum inhibitory concentration (MIC) test

The minimum inhibitory concentration (MIC) of the produced *P. major L.* extract was evaluated as the lowest concentration capable of *in vitro* inhibition against two different strains of *Staphylococcus aureus*, one susceptible (MSSA, ATCC 29213) and another resistant to methicillin (MRSA, ATCC 33591). The MIC was determined following the Performance Standards of Antimicrobial Susceptibility Testing by the Clinical and Laboratory Standards Institute in document M100, according to the method described by Mouro *et al.* 2021 [39].

2.5.2. Determination of Phenolic Compounds in *P. major* Extract

Plantago major extract solutions were prepared by solubilization of 1.0 mg/mL in ethanol/water (7:3). Subsequently, the solutions were used to calculate the concentration of total phenols and flavonoids, following the methods described by Souza *et al*. [40].

The total phenolic contents of the extracts of *P. major* were assayed by the Folin-Ciocalteu method as described earlier [40]. Quantification of total phenols was calculated using an aliquot of *P. major* solution (50 µL) and mixed with 2.5 ml of Folin-Ciocalteu reagent (1:10) and 2.0 mL of Na_2CO_3 (4%). The solution was incubated for 5 min at 50 °C. Subsequently, measurements were performed by UV-vis spectroscopy using MiliQ water as blank at 760 nm. A standard curve was obtained for gallic acid, and the phenolic content was determined from extrapolation of this curve [40]. The measurements were done in triplicate.

The total flavonoid contents of the extracts of *P. major* were determined by the aluminum chloride colorimetric method as described by Salgueiro *et al* [41]. Briefly, an aliquot of 400 µL of the extract was placed in a 10 mL volumetric flask and mixed with 200 µL of methanolic solution with $AlCl_3$ (2.0 wt. %), and completed volume, using spectroscopy grade methanol to 10 mL. The mixture was left in the dark for 30 min at room temperature, and the absorbance of the reaction mixture was recorded by a spectrophotometer at 425 nm. The measurements were made in triplicate.

The antioxidant capacity of the *Plantago major* extract was performed by the radical scavenging method (DPPH) [41]. Aliquots of 70 µL of the extract were mixed with 29 µL of 0.3 mmol/L of fresh DPPH solution and solubilized in methanol (spectroscopy grade). The final solution was incubated at room temperature and left in dark for 30 min. The absorbance of the reaction mixture was recorded at 517 nm after this time, using an ELISA plate reader (Bio-Rad, Brazil).

High-performance liquid chromatography with diode arrangement detector (HPLC/DAD) was performed with a Shimadzu Prominence Auto Sampler (SIL-20A) HPLC system (Shimadzu, Kyoto, Japan), equipped with Shimadzu LC-20AT reciprocating pumps connected to a DGU 20A5 degasser with a CBM 20A integrator, SPD-M20A diode array detector and LC solution software.). The analysis was carried out in reverse phase with column C18 (250 × 4.5 mm, 5 µm). The separation was achieved using a Betasil C18 (4.6 mm x 250 mm x 5.0 µm (Thermo) reversed-phase column held at 40 °C. The flow rate was 1.0 mL/min, and the temperature was set to 40 °C, and the injection volume selected was 15 µL. The binary mobile phase consisted of acetic acid/water (1%; A) and methanol (B) and was delivered at a flow rate of 1 mL/min. Gradient elution was performed using the following solvent gradient: starting with 85% A/15% B for 2 min, reaching 40% A/60% B in 20.00 min, then 80%B at 5 min, holding until 5.00 min, with post-time of 3 min. Detection was effected at 320 nm. The phenolic

Preprints (www.preprints.org) | NOT PEER-REVIEWED | Posted: 20 February 2023 doi:10.20944/preprints202302.0314.v1

contained in extracts analyses were recognized by comparing the retention times and the UV spectra obtained by those of the standards used.

2.5.3. Viscometry

Rheological measurements of PCL_0.0, PCL_5.3, and PCL_10.6 solutions were performed on ViscoQC-100, Rotational viscosimeter (Anton Paar Trading Co., Shanghai) using the CC18 spindle varying the shear rate at room temperature.

2.5.4. Scanning Electron Microscopy – SEM

Morphological evaluation on electrospun nanofibers with and without Plantago major extract was evaluated by SEM using a Tescan Vega3 (Brno, Czech Republic) with an acceleration of 10 kV. All samples were golden coated prior to the analysis using sputter equipment Denton Vacuum – Desk V (Moorestown, USA) for 120 seconds at 30 mA. The samples were processed using Size Meter 1.1 software for obtained the average diameters of fibers (50 measurements for each sample – n = 3).

2.5.5. Wettability assay

The contact angle analysis was used to evaluate the wettability of the PCL/*P. major* mats with the variation of hydroalcoholic extract (P. major) encapsulated, using a goniometer Ramé-Hart NRL A 100-00. A drop of distilled water (~4 μL) was deposited on the surface of each sample evaluated at room temperature. Contact angles were measured in triplicates.

2.5.6. Fourier Transformed Infrared Spectroscopy – FTIR

The incorporation of *P. major* extract in electrospun mats was confirmed using a Nicolet Fourier Transform Infrared Spectrometer equipped with an attenuated total reflectance (ATR) accessory (model 6000, Thermo Scientific). The analysis was performed in the region of 4000–650 cm^{-1}, with 64 scans and a resolution of 4 cm^{-1}.

2.5.7. Thermal Behavior by DSC and TGA/DTA

The thermal behavior of the electrospun mats was evaluated by differential scanning calorimetry (DSC) in Hitachi—DSC 7020 Thermal Analysis system equipment. Each sample (10 mg) was subjected to two heating cycles and one cooling cycle, which were carried out at a rate of 10 °C/min under a nitrogen atmosphere with a flow rate of 50 mL/min. The first heating cycle was conducted from 25 to 90 °C, followed by a cooling cycle to -80 °C and subsequent heating from -80 to 90 °C. The degree of crystallinity of the material (Xc) was calculated by Equation (1).

$$X_c = \frac{\Delta H_f}{\Delta H^o{}_f} \quad (1)$$

where ΔH_f is the melting enthalpy of the endothermic peak of the DSC thermogram (second heating), while ΔH°_f = 151.7 J/g is the theoretical melting enthalpy for a 100% crystalline PCL sample [37].

The thermal stability and weight loss of the electrospun mats (PCL_0.0, PCL_5.3, PCL_10.6) and pure dry extract were evaluated by thermogravimetry analysis using Shimadzu TGA-50 equipment with a heating range of 25 °C to 700 °C and a heating rate of 10 °C/min under N_2 atmosphere.

2.5.8. *In vitro* swelling degree

The swelling capacity of PCL and PCL/*P. major* electrospun nanofibers was performed in phosphate-buffered saline solution (PBS, pH= 7.4). The swelling degree (SD) of the samples was calculated in triplicates (n=3) using Equation (2).

$$SD(\%) = 100x\frac{W_S - W_D}{W_D} \quad (2)$$

where W_S is the weight of the swelled sample at a prescribed time and W_D is the initial mass of the sample (dry weight).

Preprints (www.preprints.org) | NOT PEER-REVIEWED | Posted: 20 February 2023 doi:10.20944/preprints202302.0314.v1

2.5.9. *In Vitro Plantago major* extract release evaluation

Plantago major L. extract delivery test from PCL electrospun mats (2x2 cm^2) was carried out in 50 mL of PBS solution (pH 7.4) at 37°C (n=3). Samples were incubated in an orbital shaker (MSM130/B, M.S. Mistura) at 70 RPM for 48 hours. Aliquots of 5 mL were collected from the medium at different periods: 0.5, 2, 4, 24, and 48 hours. The same volume of fresh PBS solution was added to the systems after aliquots removal. The amount of the extract released was evaluated by UV-Vis spectrophotometry, using a UV-Vis Perkin Elmer Lambda 25 spectrophotometer at 327 nm. In order to correlate the absorbance values with extract concentrations in the media, calibration curve of *P. major* dry extract in PBS solution was plotted. Since the addition of fresh solution alters the *P. major* extract concentration, it was corrected by using Equation (3).

$$Correction\ Factor = \left(\frac{V_0}{V_0 - V_{Aliq}}\right)^{n-1} \quad (3)$$

where V_0 is the initial volume used in the assay (V_0=50 mL), V_{Aliq} is the aliquot used in the test (5 mL), and n is the number of samples used [42].

For evaluation of extract loading and encapsulation efficiency, each electrospun mat was analyzed using a UV spectrophotometer Shimadzu (UV-2600) at 327 nm, using an accessory for thin films. The calibration curve of *P. major* dry extract in PBS solution was also used to obtain the extract concentration. The drug-loading capacity (DL) and encapsulation efficiency (EE) were calculated using Equations (4) and (5). The analysis was carried out in triplicate. The results are presented with standard deviation error (SDE) [43].

$$DL = 100x\frac{Amount\ of\ P.major\ in\ the\ PCL\ electrospun\ mat}{Amount\ of\ the\ PCL\ electrospun\ mat} \quad (4)$$

$$EE = 100x\frac{Amount\ of\ P.major\ in\ the\ PCL\ electrospun\ mat}{Amount\ of\ the\ P.major\ initial} \quad (5)$$

2.5.10. Antimicrobial assay of *P. Major*

For antimicrobial analysis of the hydroalcoholic extract, two bacteria were used, one gram-negative *Escherichia coli* (CECT 434) and the other gram-positive *Staphylococcus aureus* (CECT 86). The strains were stored in Tryptone Soy Broth (TSB, Scharlab) with 20% glycerol at -80 °C. The culture broth was maintained in STA-agar solution at 4 °C, following the method used with modifications by Calatayud et al. [44] Each strain was transferred to 10 ml of TSB and incubated at 37 °C for 18 h to obtain cells in initial stationary phase.

Cell cultures were performed in the stationary phase, with an optical density of 0.9 at 625 nm. The bacteria culture was diluted in TSB and incubated at 37 °C under an optical density of 0.2 at 625 nm (10^5 CFU/ml) in exponential phase 100 µL of Mueller Hilton Brith (MHB, Scharlab). Samples of the mats with approximate mass of 35 mg (1.0 cm in diameter) were placed in each of the tubes and incubated at 37 °C for 18 h. A tube with PCL_0.0 mat was used as positive control, while the hydroalcoholic extract deposited on filter paper (1.0 cm in diameter) and dry posteriorly for used as negative control (Method adapted from CLSI M07-A9) [45].

3. Results and discussion

3.1. Composition evaluation of Plantago Major extract.

Flavonoid and phenolic compounds are the main secondary metabolites identified for the application of plants in medicine and pharmaceutical applications. These compounds are considered effective antimicrobial and antioxidant sources. Therefore, identification of these chemicals is very important when natural products from parts of plants such as seeds, leaves, and others are used in pharmaceutical applications.

Preprints (www.preprints.org) | NOT PEER-REVIEWED | Posted: 20 February 2023 doi:10.20944/preprints202302.0314.v1

Total phenolic (TP) compounds present in the *P. major* freeze-dried extract was determined as 65.4 ± 0.002 mg GAE/g, a value close to those recorded in the literature for ethanolic extract of this plant (65.53 ± 0.034 mg/g). However, this result was twice higher as for the hydroalcoholic extract (32.12 ± 2,75 mg/g), which was the same extraction solvents used in this work [41]. The phenolic compounds are capable of neutralize free radicals, activate anti-oxidant enzymes, among other metabolic activities etc. [46].

The total flavonoid (TF) content was determined by the aluminum chloride complexation method which is specific for flavones and flavanols. An analytical curve of quercetin was used as standard (R^2 = 0.99) for quantification. The TF results for the *P. major* freeze-dried extract were quantified as 5.7 ± 0.001 mg/g (EQ). However, this valor is 5 times lower than values reported in the literature for flavonoids in ethanolic extract (28.76 ± 1.05 mg/g EQ) and 3.5 times lower (19.93 ± 0.51 mg/g EQ) for the hydroalcoholic extracts [47].

The antioxidant effect of *P. major* extract was evaluated by DPPH scavenging due to its ability to scavenge DPPH free radicals by hydrogen donation. The activity was expressed in µg/ml and represents the concentration of the extract needed for 50% inhibition of free radicals (IC_{50}). On the other hand, it was reported that a lower IC_{50} indicates higher activity in this assay. It was found that the IC50 of the hydroalcoholic extract produced in this work is 14.55 µg/ml. (r^2 = 0.99; n = 4), demonstrating a high ability to reduce the stable radical and exhibit effective scavenging activity compared to the antioxidant capacity of *P. major* extracts extracted with different solvents. Karima et al. (2015) evaluated that the *P. major* extracts obtained with ethyl acetate (Ac) presented strong antioxidant activity (IC_{50} of 12.85 ± 0.27 µg/ml), while those obtained with aqueous extract (Aq) showed low light activity (IC_{50} of 109.67 ± 0.21 µg/ml). Moreover, the extract produced from petroleum ether fraction (PE) presented even lower antioxidant capacity (439.84 ± 6.51 µg/ml). Thus, it is possible to say that the extract produced in this work offers an effective antioxidant power since the IC_{50} is close to the IC_{50} recorded for Ac [48]. The high antioxidant activity may be attributed to the high phenolic content. Extracts with high antioxidant capacity have been shown to facilitate the wound healing, since they can remove the products of inflammation in wound bead, i.e., the excess of proteases and the reactive oxygen species (ROS) [49].

Studies reported in the literature demonstrate a direct relationship between the various components of natural extracts used in traditional medicine and their applicability. For example, secondary metabolites such as *squalene*, and *docosan*, which are responsible for the anti-inflammatory and antimicrobial activity respectively, are found in extracts produced from leaves of medicinal plants such as *Plantago major L* [29,50,51]. Based on this fact, the identification of secondary metabolites in the extract produced in this study is of most importance. For this reason, the freeze-dried hydroalcoholic extract was evaluated by HPLC and the chromatogram is presented in Figure 1. *Plantago major L.* extract is rich in tannins, flavonoids, caffeic acid, and other substances that demonstrate its efficacy to be used on skin wounds, which generates its antimicrobial and antifungal action [25].

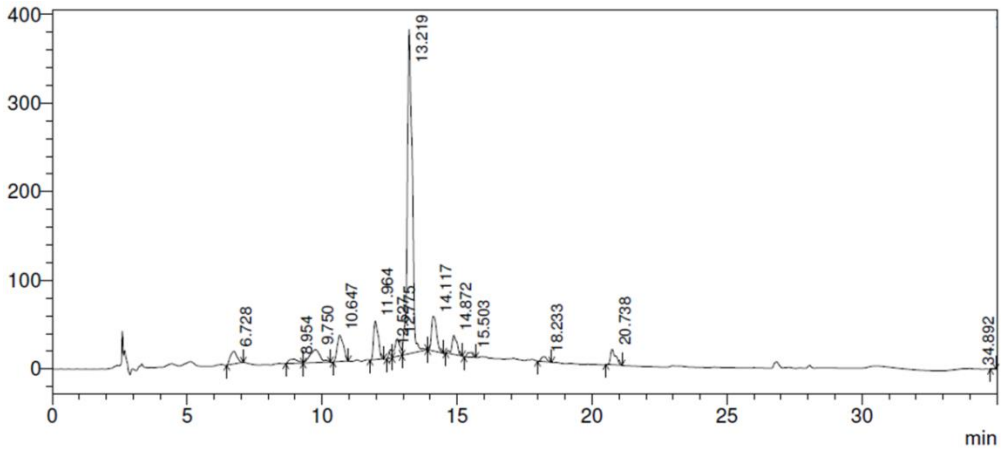

 doi:10.20944/preprints202302.0314.v1

Figure 1. HPLC chromatogram from *P. major* extract obtained by C-18 column (250 mm x 4.6 mm x 5 µm), flow rate 1.0 mL/min, and mobile phase composed by water: acetic acid (99:1, solvent A) and methanol (Solvent B) at 320 nm.

3.2. *Minimal inhibition concentration (MIC) evaluation*

Figures 2 and 3 show the results of the minimum inhibitory concentration assay of *Plantago major* extract against two different strains of *Staphylococcus aureus*, one susceptible (MSSA) and another methicillin-resistant (MRSA). *S. aureus* is a gram-positive opportunistic bacteria that colonizes the skin lesions, hampering wound-healing processes and increasing the severity of the lesions. It is often associated to nosocomial infections. Recently, the MRSA was indicated as the one of the leading pathogens responsible for patients death related to antimicrobial resistance. In 2019, more than 100,000 deaths were attributed to this lineage [52].

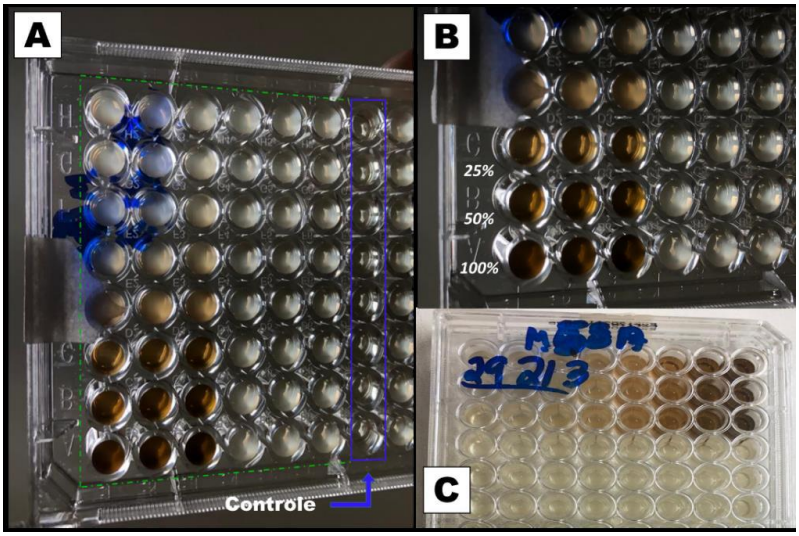

Figure 2. Inhibitory dose study in microplates with dilution for MSSA *S. aureus*. A) Photograph of the bottom of the microplate highlighting the wells with the control group and the 48 wells with the extract using the methicillin-susceptible *S. aureus* strain (MSSA). B) Enlarged photograph for the wells with 100, 50, and 25% of the extract. C) Photograph of the top of the plate with the bacterial strain (MSSA).

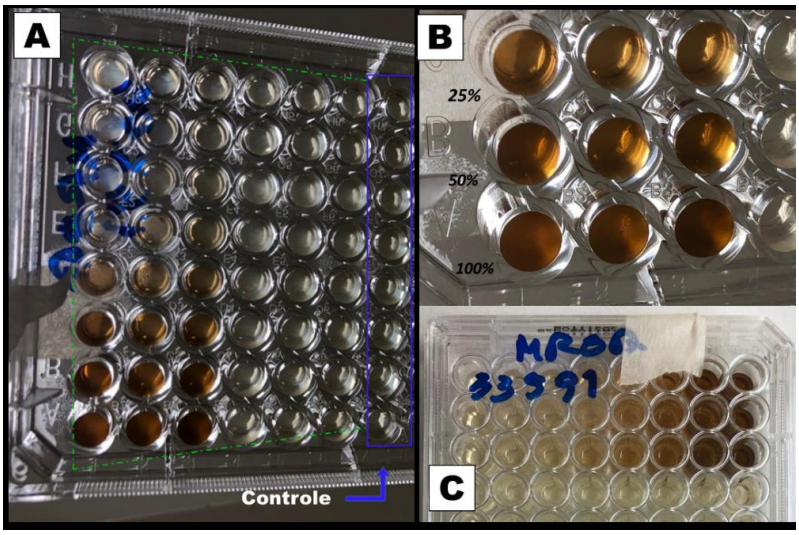

Figure 3. Microplate inhibitory dose study for resistant *S. aureus* (MRSA). (a) Photograph of the bottom of the microplates highlighting the wells with the control group and the 48 wells with the

Preprints (www.preprints.org) | NOT PEER-REVIEWED | Posted: 20 February 2023 doi:10.20944/preprints202302.0314.v1

extract. (b) Enlarged photograph for the wells with 100, 50, and 25 % of the extract. (c) Photograph of the Upper part of the plate with the type of bacteria (MSRA).

For this test, a liquid medium was introduced in wells of a microplate and, through successive dilutions, the minimum concentration of the extract that inhibits bacterial growth after 48 h of culture was determined. The solution in the wells that contain the control group (culture medium without inoculum) remained clear after incubation, which indicates that there was no external contamination during the experiment. For both, the MSSA (Figure 2) and MRSA (Figure 3) strains inhibition occurs for a concentration of 25% (v/v), which represents a concentration of 5.3 mg/mL of dry mass calculated from 10 mL of fresh extract, since these wells also present clear solutions. On the other hand, for lower concentrations, a turbid deposition was observed at the bottom of the microplate wells, indicating the proliferation of the bacteria in the medium [28]. For this reason, the PCL/*P. major* electrospun nanofibers was produced from solutions containing 5.3 mg/mL of the extract (MIC) and 10.6 mg/mL (2 x MIC).

3.3. *Viscosity evaluation*

One of the main variables that influences the morphology of electrospun nanofibers is the viscosity of the solution to be spun. This is attributed to the ability of entanglement of the polymer chains that will allow their interaction during the spinning process [53]. The viscosity of PCL solution (10 wt. %) with different content of *P. major L.* extract was performed at different shear rates (Figure 4). The studied solutions was PCL_0.0 (pure PCL 10 wt%), PCL_5.3 (PCL 10 wt% plus *P. major* at MIC concentration), and PCL_10.6 (PCL 10 wt% plus *P. major* at twice MIC concentration).

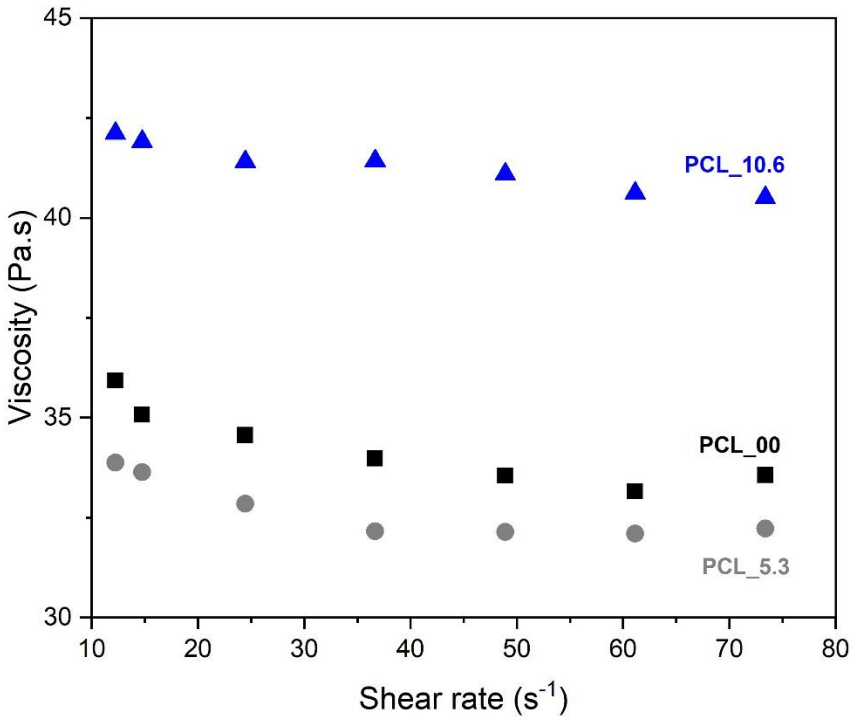

Figure 4. Rheological behavior of PCL solutions with different contents of *Plantago major* dry extract.

The three solutions show Newtonian behavior. As shown in Figure 4, the solution of PCL without extract (PCL_00), and that of PCL with 5.3 wt. % of extract (PCL_5.3) presented similar viscosity values throughout the range of shear rate tested. A slight viscosity reduction was observed for the solution with lower extract concentration (5.3 wt. %) in relation to that of the pure PCL solution, which may be related to a lubricant behavior of the molecules of the extract inside the polymeric network. This behavior was also observed in the results presented by Figueiredo *et al.* (2022) [54], who observed the lubricant behavior on viscosity when incorporating propolis extract into the PCL solution.

 doi:10.20944/preprints202302.0314.v1

On the other hand, this behavior was not observed for the solution with the highest extract content (PCL_10.6), which showed an 18% increase in viscosity values as compared to the pure PCL solution. This result may be related to a possible supersaturation of the solution, creating a suspension that affects the chemical interaction/affinity with the polymer [55].

3.4. PCL/P. major electrospun samples

The PCL spinning study of this work started based on previous studies developed in our research group [37,54], with variations of solvent systems. The solution was prepared using PLC (10 wt. %) in DCM/DMF. Studies were performed to select the suitable experimental parameters to obtain fibrillar morphology without defects and with smaller and more homogeneous fiber diameters (data not shown). Based on this investigation, the following spinning conditions were chosen: flow rate = 0.75 m/h; voltage = 17 kV; needle tip–collector distance = 12 cm. Three solutions were spun using a 5 mL solution with different *P. major* extract concentration, pure PCL (PCL_00, PCL_5.3 and PCL_10.6).

Figures 5a,b present the fibrillar morphology of neat PCL (233.2 ± 84.2 nm) and with 5.3 wt. % extract (235.5 ± 72.2 nm), respectively. It shows that by adding this proportion of the extract in PCL did not significantly change the average diameter and fiber's morphology which was maintained with no significant presence of defects and beads for both samples. However, for the higher concentration of *P. Major* in PCL (10.6 wt. %) (Figure 5c), a higher average diameter and a large distribution of diameters were observed in the fibers (378.5 ± 118.5 nm). These variations may be attributed to instabilities in the solution with the addition of higher amount of the extract, which could be related to the occurrence of a phase separation during the spinning processing due to the difference of polarity between PCL and extract or to the supersaturation of the solution as suggested before. Analysis of Variance (ANOVA) Post Hoc Test - Fisher's Least Significant Difference (LSD) (calculated LSD = 0.877) indicates that increasing levels of P. major extract on the electrospun solution were statistically significant from 0 to 10 wt. % (LSD > $1.5x10^{-12}$), and from 5 to 10 wt. % (LSD > $1.5x10^{-12}$). However, the increment of 5 wt. % of vegetal extract concerning the pure PCL solution (LSD < 0.899) was not influential for the fiber diameter.

Preprints (www.preprints.org) | NOT PEER-REVIEWED | Posted: 20 February 2023 doi:10.20944/preprints202302.0314.v1

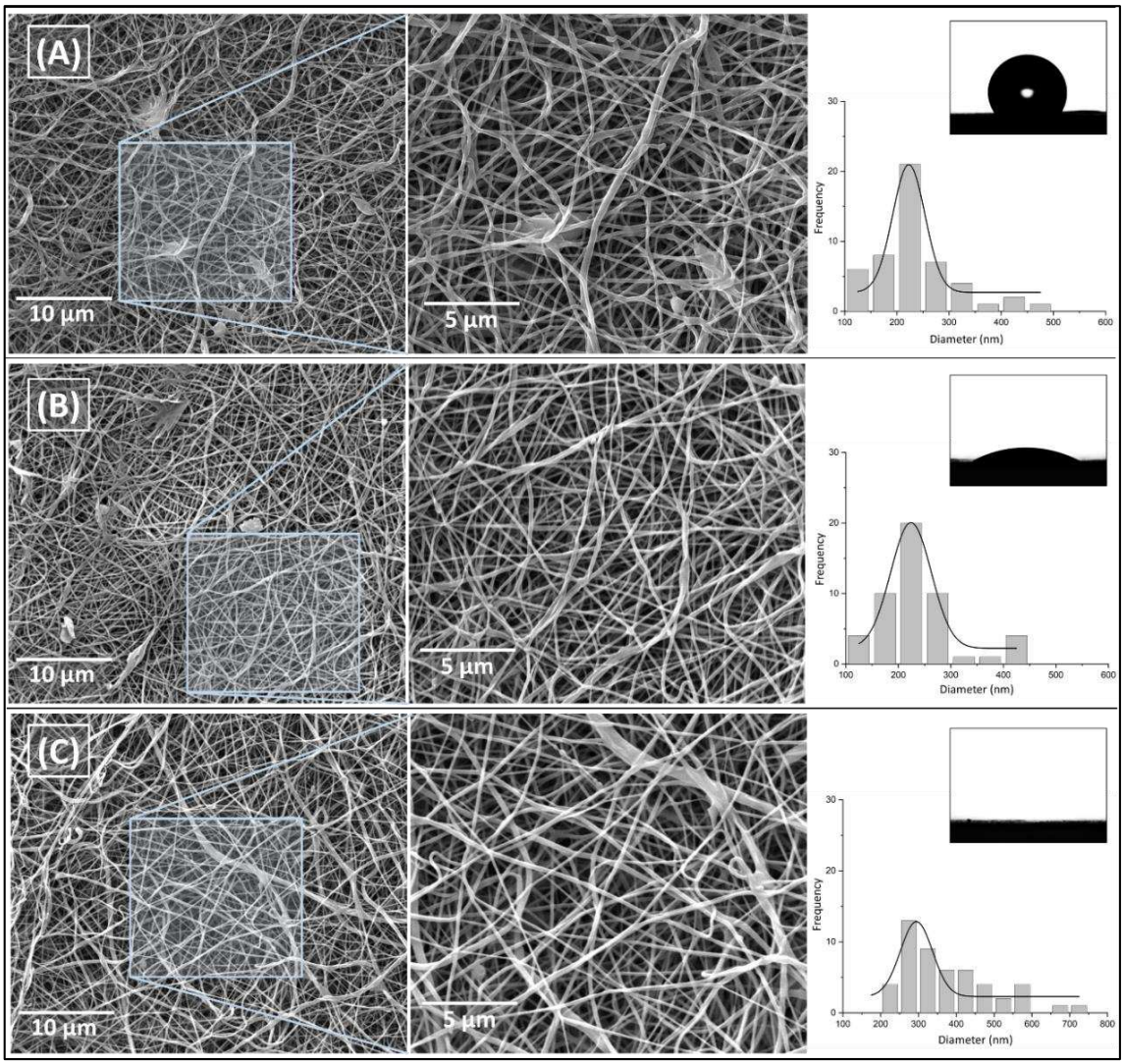

Figure 5. SEM images of electrospun mats with magnification variation and their histograms varying concentrations of *P. major* extract in the relationship of PCL and the image of water drop on the surface of the mat that was taken during contact angle (CA) analysis. A) PCL nanofibers without extract (PCL_00%); B) PCL nanofibers with 5.3% of the extract (PCL_5.3%), and C) PCL nanofibers this 10.6% of the extract (PCL_10.6%).

To evaluate the incorporation of the extract in the polymer matrix (PCL), the wettability test was performed on the surface of the electrospun mats. The image of the water drop on the surface of each mat was shown in Figure 5a–c. The results indicate a decrease in the contact angle of the mats formed by fibers containing the *P. major* extract, from 121.9° for neat PCL to 39.4° and 0° when the extract concentration is increased. The wettability is mainly related to the surface chemical interactions of the material as well as its morphology [53,55]. As shown in Figure 5, PCL_00 and PCL_5.3 samples presented fibrillar morphology with very similar fiber diameters, which mainly demonstrates that the variation of the contact angle for these samples may be related to the incorporation and functionalization of PCL nanofibers by the extract and the arrangement of the polar groups on the surface of the produced nanofibers [56]. The *P. major* extract has halogenated and OH-containing components, which makes it rich in hydrogen bonds, and with a large affinity to water, unlike PCL, which is a highly hydrophobic polymer. On the other hand, the PCL_10.6 sample, which showed total water absorption (CA = 0°), may be influenced by the two main phenomena, one related to the chemical character/composition of the extract, as well as, the capillarity of the mats, since a possible increase in the pores formed inside the fibers was verified. This feature generates a higher humectability capacity of their fibers compared to the other two samples evaluated [54,58]. It is well-

Preprints (www.preprints.org) | NOT PEER-REVIEWED | Posted: 20 February 2023 doi:10.20944/preprints202302.0314.v1

known that a material with hydrophilic character may provide conditions for cell attachment, proliferation, migration, and differentiation.

3.5. Fourier transformation infrared – FTIR

Figure 6 presents the FTIR-ATR spectra of PCL electrospun mats and the freeze-dried *P. major* extract following reports in the literature [59], it was able to easily identity in the PCL spectrum the band attributed to carbonyl group stretching (C=O) at approximately 1750 cm^{-1} [42]. Absorption bands related to the solvents used in the electrospinning process were not found, being possible to state that, if present, the solvents are in very low quantity in the fibers having been evaporated almost completely during the spinning process.

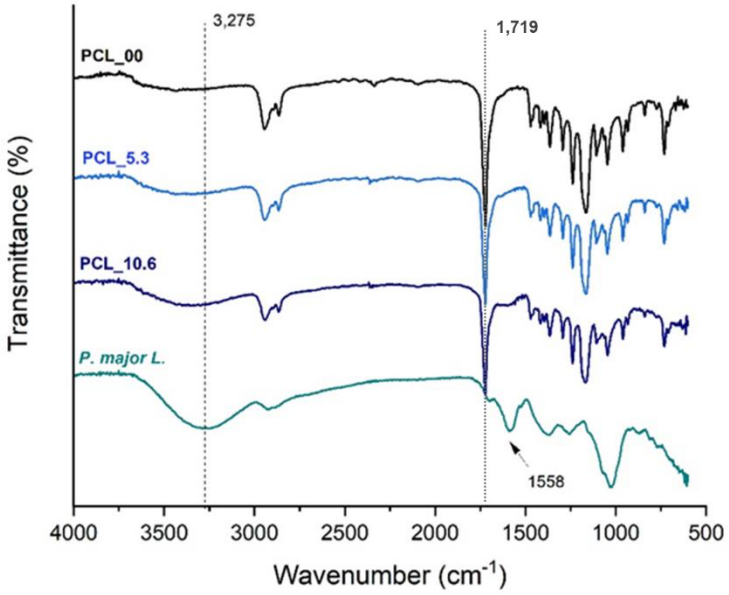

Figure 6. FTIR-ATR spectra of the PCL electrospun mats with different amounts of *Plantago major* extract and the freeze-dried extract.

The spectrum of the extract shows a broad band at 3275 cm^{-1} which is characteristic of the vibrations of phenolic groups and O-H bonds of polyphenols and flavonoids. It was also observed the presence of a band at 1719 cm^{-1} due to C=O bond also present in polyphenols and flavonoids of the *P. major* extract [35,60,61]. A characteristic band of *P. major* at 1558 cm^{-1} was observed in the FTIR spectra of PCL_5.3 and PCL_10.6 samples, demonstrating the incorporation of *P. major* extract in the polymer nanofibers [62-64]. The incorporation of the extract in the fibers was corroborated since the transmittance band of the carbonyl characteristic of PCL (C=O) at 1719 cm^{-1} had a slight shift to higher values of 1723 cm^{-1} for PCL_5.3 and 1726 cm^{-1} for the sample with 10.6 wt. % (PCL_10.6), which can be attributed to the formation of intermolecular hydrogen bonds between PCL and the *P. major* extract [35,65].

3.6. Thermal behavior of electrospun mats

The thermal behavior for the three samples evaluated in this study was characterized by DSC (Figure 7) and TGA with the aim that evaluating the influence of *P. major* extract on the thermal transitions and thermal stability of PCL for each sample. Values of melting temperature (T_m), enthalpy of melting (ΔH_m), and degree of crystallinity (Xc) are shown in Table 2.

Table 2. Melting temperature and crystallinity degree of electrospun mats of PCL/*P. major*.

Sample	1st heating cycle			2nd heating cycle		
	T_m [°C]	ΔH_m[J/g]	Xc	T_m [°C]	ΔH_m [J/g]	Xc

Preprints (www.preprints.org) | NOT PEER-REVIEWED | Posted: 20 February 2023 doi:10.20944/preprints202302.0314.v1

PCL_0.0	55.4	123.0	81.1	51.4	117.0	77.1
PCL_5.3	55.4	80.5	53.1	51.1	74.2	48.9
PCL_10.6	54.3	88.5	58.3	50.6	86.0	56.7

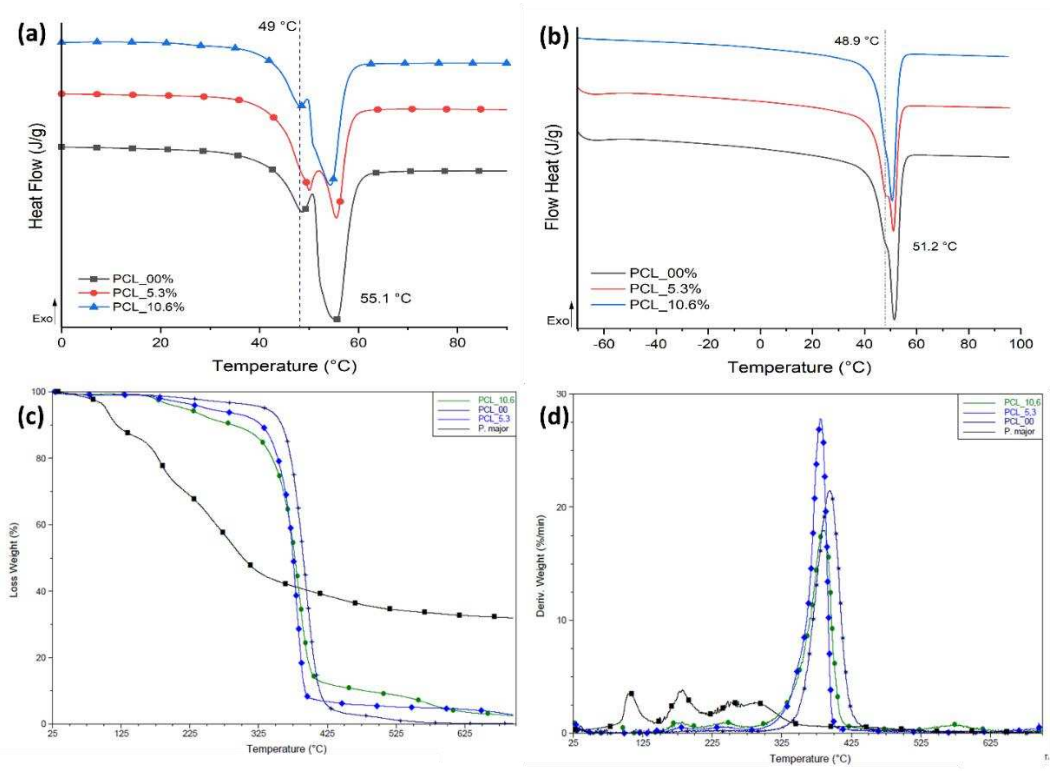

Figure 7. Thermal behavior PCL/*P. major* electrospun samples: DSC curves for electrospun mats from PCL with different concentrations of *P. major* extract. (a) First heart cycle and (b) Second heat cycle; TG (c) and DTG (d) curves.

The electrospinning process generates rapid elongation of polymer chains that allow their alignment, promoting high structural organization [66], and degree of crystallinity than that measured in the second heating cycle as shown in Figure 7a. However, this process can regenerate variations in the population of crystalline lamellae that are evidenced in the first heating cycle as two main types of crystals: one less perfect melting at 49 °C approximately, and a second population (in larger proportion) evidenced by a higher ΔH_m at 55.1 °C. The same behavior was seen for samples with two different natural extract contents.

For the second heating cycle, Figure 7b, the PCL electrospun mats with the *P. major* extract showed a decrease of approximately 36.6 % in the degree of crystallinity of the fibers with 5.3 wt.% of the extract compared with PCL fibers without the extract (PCL_00) (Table 2). This demonstrates an interaction between freeze-dried extract and PCL chains that can be attributed to the fact that the *P. major* molecules were able to allocate themselves between polymer chains, promoting the increase in the space between them, and increase in the difficulty of these chains in reorganizing as ordered crystal structures [54,67]. Nevertheless, this large decrease in the degree of crystallinity was not observed when the concentration of the extract was increased to 10.6 wt.% (PCL_10.6), and a slight increase in crystallinity was observed with relation to PCL_5.3. This can be attributed to a possible supersaturation of the extract solution which creates phase separation in the solution, resulting in a low homogeneity or dispersion of the extract in the electrospun nanofibers. Although PCL_10.6 has lower Xc compared to the neat PCL fibers (PCL_00), it has Xc about 16 % higher than sample PCL_5.3.

Figure 7c,d shows TG and DTG curves of the PCL/*P. major* electrospun mats which allow to infer about the thermal stability of the samples. Three stages of mass loss are evidenced for the *Plantago major* extract. The first stage occurs between approximately 60-150 °C and is attributed to loss of the water present in the sample [35]. This stage was not observed in any electrospun sample,

 doi:10.20944/preprints202302.0314.v1

demonstrating absence of small molecules like water and solvent in the nanofibers (Figure 4c). However, three stages of mass loss at higher temperatures were seen in the PCL/*P. major* electrospun mats, two of them with maximum DTG mass loss rate (peak maximum) at 181 and 256 °C, attributed to components of extract, and one between 320-450 °C related to the stage of PCL chain degradation [54,68].

3.7. In vitro swelling behavior of electrospun nanofibers

Keeping a moist environment in the wound is of great importance to promote the different stages of tissue regeneration, favoring the formation of granular tissue, thus accelerating re-epithelization in the first 48 hours after dressing application [69]. Another important feature in the implementation of dressing for skin, besides keeping this moisture, is the non-retention of the absorbed exudate and fluids excessively, creating maceration in the tissue surrounding the wound [70].

Figure 8 shows the degree of swelling of the electrospun mats evaluated in this study. PCL/*P. major* electrospun mats were immersed in PBS (pH 7.4) for 96 hours. Subsequently, the samples were freeze-dried and analyzed by SEM (Figure 8c–e). The comparative diameters of fibers before and after the swelling/release assay and the mass variation of mats were shown in Table 3.

Electrospun mats have a high contact area and porosity attributed to their fibrillar morphology. This allows the surrounding medium (PBS) to penetrate the mat due to capillary effects, independent on the hydrophobic character of PCL as observed in the contact angle evaluation (Figure 8). Where the pure PCL fibers (PCL_00) showed a PBS absorption capacity of ~22 % for the first hours (Figure 6b), as well as a constant increment during the test up to approximately 200 % a result that agrees with the results shown in the literature for electrospun pure PCL fibers [71]. On the other hand, this behavior was not observed for the samples with *P. major* extract. It was shown to have a higher swelling capacity. This can be attributed to the location of the extract on the surface of the fibers allowing better interaction mat/PBS.

Table 3. Comparative diameters and mass variation after assay of the electrospun nanofibers before and after swelling with lyophilized electrospun mats.

Sample	Fiber diameters [nm]		Mass Variation
	Before	After	[%]
PCL_00	233.2 ± 84.2	258.3 ± 77.8	3.7 ± 0.38
PCL_5.3	235.5 ± 72.2	261.9 ± 84.4	7.1 ± 0.15
PCL_10.6	378.5 ± 118.5	428.1 ± 136.9	30.4 ± 10.2

Preprints (www.preprints.org) | NOT PEER-REVIEWED | Posted: 20 February 2023 doi:10.20944/preprints202302.0314.v1

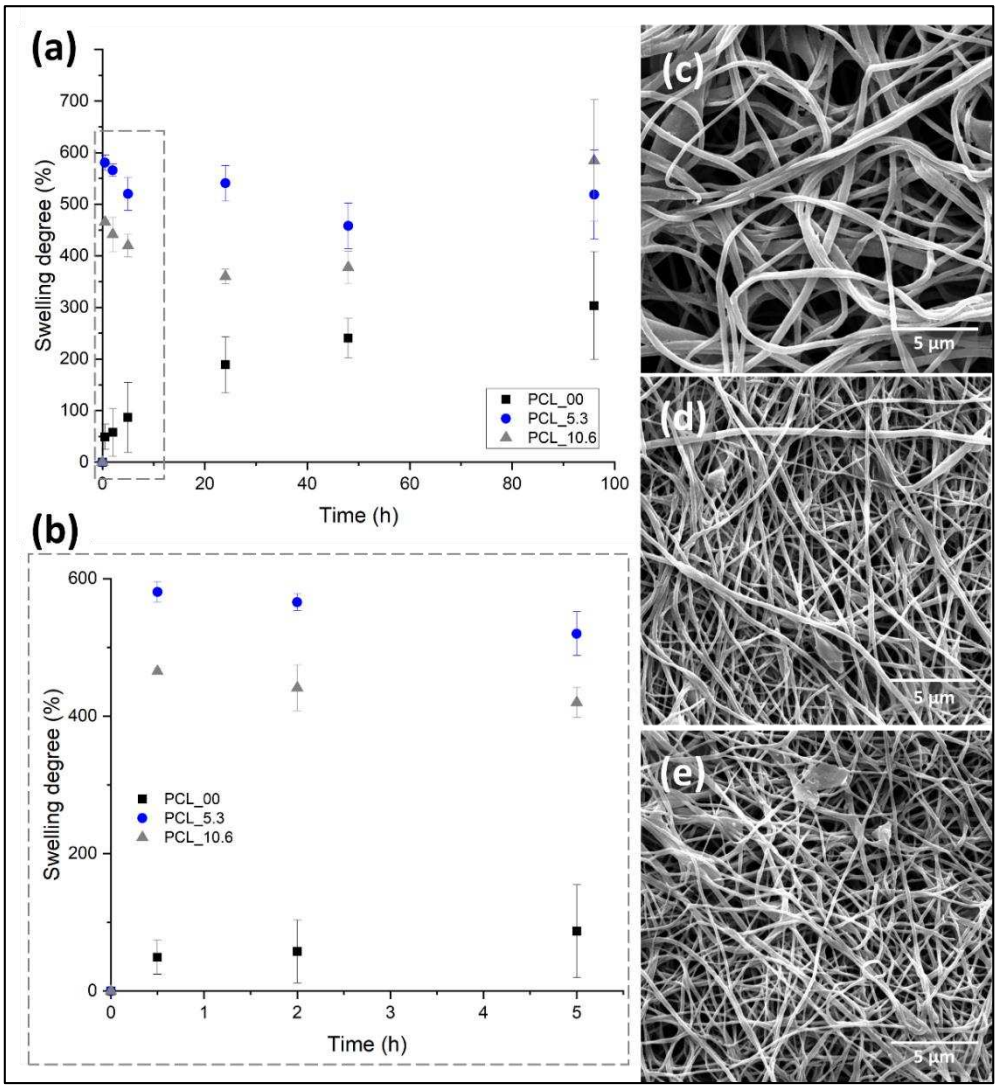

Figure 8. Degree of swelling for PCL/*P. major* electrospun mats as function of the immersion time in phosphate buffer solution – PBS (pH: 7.4): (a) 96 hours of the assay, (b) first 5 hours of swelling assay; SEM images of *PCL/P. major* electrospun mats after swelling assay (96 h): (c) PCL_10.6; (d) PCL_5.3, and (e) PCL_0.0.

As seen in Figure 8, the incorporation of the extract increased the medium adsorption capacity of the nanofibers. For example, in the first hour PCL_10.6 samples had 465 % of swelling degree and the samples with 5.3 wt. % (PCL_5.3) of the *P. major* extract had 580 %, evidencing that the incorporation of the extract generated hydrophilicity characteristics and higher wettability compared to the neat PCL fibers (PCL_00). This behavior can be attributed to the hydrophilic components present in the extract. It is important to mention that a higher adsorption capacity was observed for the electrospun fibers with 5.3 wt. %, which had this swelling behavior maintained during the 96 hours test in PBS.

Subsequently to the swelling test, the samples were weighed, and the morphology obtained from SEM images compared with the initial nanofibers. The results of mass variation and fiber's morphology (Table 3 and Figure 8c–e) suggested that no degradation of the electrospun PCL fibers by the PBS medium took place for both materials, with and without the extract. Although a low mass variation was observed for PCL_00 mat after the swelling test in PBS, it seems that small quantity of salts present in the liquid medium was absorbed by the hydrophobic PCL.

On the other hand, the fiber diameter showed significant variation after the swelling test (freeze-dried), even for the neat PCL fibers. The fibers showed diameter increase of approximately 10.7%, 11.2%, and 13.1 % for the PCL_00, PCL_5.3, and PCL_10.6, respectively, demonstrating the absorption

Preprints (www.preprints.org) | NOT PEER-REVIEWED | Posted: 20 February 2023 doi:10.20944/preprints202302.0314.v1

capacity after 96 hours submerged in PBS. The result is in concordance with reports made in the literature for PCL/propolis electrospun mats, which demonstrates the ability to maintain the moistness of the wound for its recovery [42,54].

3.8. P. major extract encapsulation

The capacity of encapsulation of P. major extract in PCL by electrospinning was evaluated by UV-Vis spectroscopy using a thin film accessory. It was evaluated by two methods: the drug-loading capacity (DL), which is the amount of drug loaded per unit weight of each mat, and the Encapsulation Efficienty (EE), which describes the concentration of the active material incorporated on electrospun mats, relationship with the initial P. major extract amount placed into the polymeric solution [43]. The result is shown in Table 4.

Table 4. *Plantago major* loading capacity and encapsulation efficiency in PCL nanofibers (n=3).

Sample	Drug-loading Capacity (DL)		Encapsulation Efficiency (EE)	
	Theoretical [%]	Experimental [%]	Theoretical [%]	Experimental [%]
PCL_5.3	25	13.02	~100	63.52
PCL_10.6	50	31.01	~100	60.31

We have found that the experimental DL of *P. major* in nanofiber's mats was aproximately 50% of what would be expected theoretically. Similar behavior was observed for experimental EE, where it showed minor values (~40%) compared with the theorical value. This result can be attributed to the chemical characteristic different between PCL-*P. major* extract generating some instability of extract in the polymeric solution as mentioned previously. This was corroborated with the variation of the amount *P. major* extract put on solution, increasing the instability in the polymeric solution, forming fibers with major variation in the extract concentration. This result in decreasing in the encapsulation amount as show in the Table 4, for EE.

3.8. P. major extract release assay

To evaluate the delivery of the encapsulated extract, release assay of electrospun PCL nanofibers was performed in PBS (pH 7.4) at 35 °C under stirring (100 rpm). Aliquots were taken at different times up to 48 h. The release was quantified using UV-Vis spectrophotometer. Quantifications of *P. major* extract release were evaluated for the two different *P. major* concentrations, 5.3 and 10.6 wt. % (Figure 9).

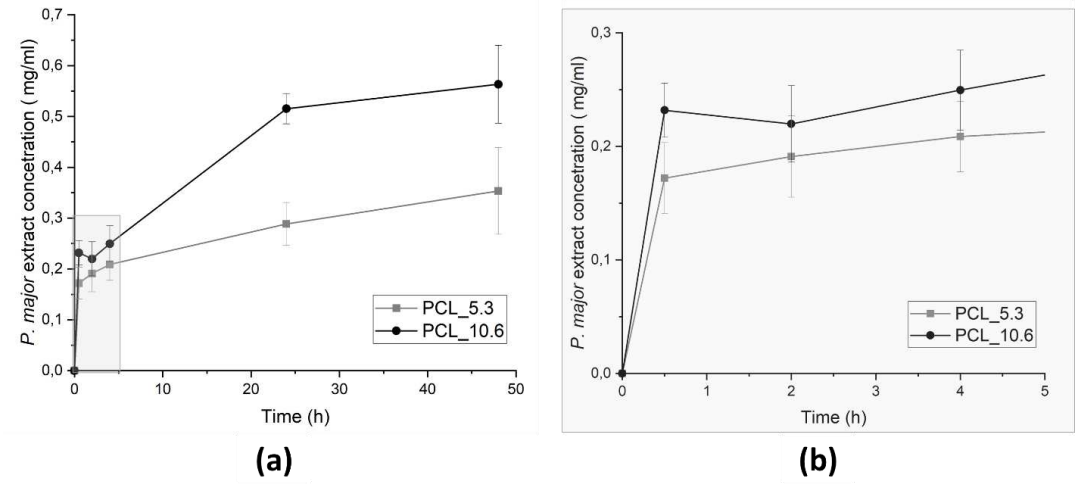

Figure 9. *P. major* extract release from PCL/*P. major* electrospun mats as function of the immersion time in phosphate buffer solution – PBS (pH 7.4): (a) 48 hours of assay, and (b) zoom of the evolution of the release assay in the first 5 hours.

Preprints (www.preprints.org) | NOT PEER-REVIEWED | Posted: 20 February 2023 doi:10.20944/preprints202302.0314.v1

The highest speed of extract release was achieved in the first 24 hours of assay, which is a significant result considering the use of these materials in wound dressing, since clinically the time of using a dressing may not exceed 24 hours. This occurs because the adsorption of exudate generates bad odors and discomfort to patient and health staff.

The delivery profile from monolithic nanofibers showed more controlled release, since burst effect characteristic of electrospun nanofibers was not observed. The maximum delivery rate of the extract was observed after the first 24 hours of assay for both concentrations of the encapsulated extract [66,72].

Figure 9 also presents the cumulative delivery of *P. major* extract in PBS which shows deliveries of 0.17 mg/ml and 0.23 mg/ml in the first minutes of the assay (30 min), and a total delivery of 0.35 mg/ml and 0.56 mg/ml for PCL_5.3 and PCL_10.6, respectively, after 48 h assay. These values are within the values recorded for bacterial inhibition reported in the literature (Grand-negative, and fungus) for studies using *P. major* extracts from leaves (between 0.1 and 1.0 mg/ml) [22,73].

3.9. Antimicribial assay from PCL/P. major electrosun nanofibers

One of the most relevant properties cited in the literature for *P. major* is the content of flavonoid, tannins, phenolics compounds among other substances that contribute to its antimicrobial action for leaves and stem, as well as for the seeds in the preparation of the mucilage [74].

Figure 10 shows the results of antimicrobial activity of *P. major* extract and PCL_5.3 electrospun mats. As positive control, samples of neat PCL (PCL_00) mats were used. For the negative control, the lyophilized extract on filter paper and dry was used.

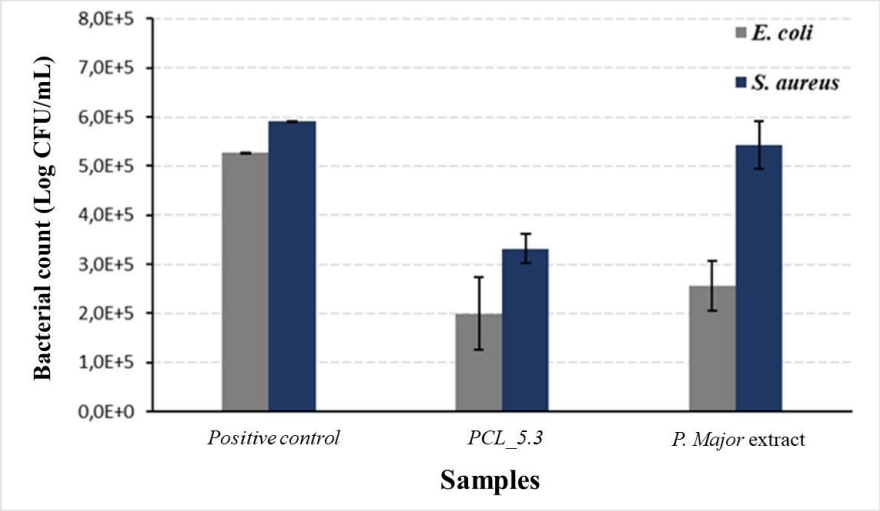

Figure 10. Antimicrobial activity of *Plantago major* hydroalcoholic extract and PCL/*P. major* electrospun mat against *E. coli*, and *S. aureus* strains. Pure PCL electrospun mat (PCL_0.0) was used as positive control.

This study demonstrated the capacity of the *P. major* extract to eliminate *E. coli*, as shown in Figure 10. The Figure also show that the action of the pure extract against *S. aureus* was not so significant with an only slight decrease in the bacterial count when compared to the positive control. The low antimicrobial activity of the pure extract may be related to its low content of total flavonoids, as discussed before. This result agrees with the literature, which reports that the hydroalcoholic extract shows the highest inhibition for gram-negative bacteria [75,76]. The antimicrobial assay showed, however, that for the PCL/*P. major* sample the decrease in proliferation of both *E. Coli* and *S. Aureus* bacteria strains was approximately 60%. It was not observed any complete inhibition for the used strains, result that agrees with those recorded in the literature [77,78]. On the other hand, this partial inhibition can be explained considering possible interactions between the extract and the polymer that did not allow the complete release of the extract, as shown in Figure 9, avoiding the

achievement of the minimum inhibitory concentration of these strains. Thus, other studies are necessary to evaluate the release of other concentrations of the extract that can inhibit these bacteria strains.

4. Conclusions

In this study, mats of nanofibers of PCL with 5.3 and 10.6 wt.% of *Plantago major L.* extract was successfully produced by monolithic electrospinning. Fibrillar structures with homogeneous diameters of about 230 nm and beads free were obtained. The viscosity of the solution with 5.3 wt. % *P. major* presented a slight reduction due to a lubricant effect of the extract molecules, while the solution with 10.6 wt. % presented a significant increase in viscosity which may be related to possible emulsification of the extract. A significant influence of the extract on the morphology and diameters of the electrospun fibers has occurred, especially for the material containing 10.6 wt. % of the extract ($P < 0.05$). The incorporation of the extract in PCL improve the wettability of the samples clearly seen by the decrease in the contact angle, mainly due to the presence of the extract on the surface of the electrospun fibers. The interaction between *P. major* extract and PCL was verified due to a slight shift of the carbonyl group infrared absorption band (~1700 cm^{-1}) to lower values, which probably hindered the release of the total amount of the extract to the medium. The in vitro swelling and drug delivery assays demonstrated its potential application as a bioactive dressing for cutaneous wounds, due to its power to retain moisture inside the matrix in approximately 500%, and extract release between 0.2 to 0.5 mg/ml, values in in the range for effective biological activity in cell assays. The nanofibrous mats also presented an adequate delivery speed to promote tissue repair. In summary, this delivery system has potential to be used as functional dressing for the recovery of difficult-to-heal skin lesions, since it combines the antimicrobial and antioxidant capacity of *P. major* extract with the special properties of PCL nanofibers, such as its capacity of mimic the morphology of extracellular matrix of skin, which provide suitable environmental to cellular repair, and the presence of interconnected pores that promotes a physical barrier to avoid contamination of the wound bed and facilitates nutrients exchanges and the exudate absorption.

Author Contributions: Conceptualization, M.L.D., and R.M.S.M.T.; methodology, J.M.A.M., V.M.Q., V.S.C., A.B.V., R.F.S., R.N.C.; validation, J.M.A.M., V.M.Q., A.B.V., and R.F.S.; formal analysis, J.M.A.M., V.M.Q., V.S.C., A.B.V., R.F.S., and R.N.C.; investigation, J.M.A.M., V.M.Q., V.S.C., A.B.V., R.F.S., and R.N.C.; data curation, J.M.A.M., V.M.Q., V.S.C., and R.F.S.; writing—original draft preparation, J.M.A.M.; writing—review and editing, M.L.D., and R.M.S.M.T.; visualization, J.M.A.M., and R.N.C.; supervision, M.L.D., and R.M.S.M.T.; project administration, M.L.D, R.M.S.M.T.; funding acquisition, M.L.D., and R.M.S.M.T. All authors have read and agreed to the published version of the manuscript.

Funding: The authors are grateful to the following Brazilian agencies: Coordenação de Aperfeiçoamento de Pessoal de Nível Superior – CAPES, National Council for Scientific and Technological Development – CNPq (Grants 308789/2020-2, 307364/2018-6, and 312851/2017-0), and Fundação Carlos Chagas Filho de Amparo à Pesquisa do Estado do Rio de Janeiro – FAPERJ (Grants: Temáticos – E-26/211.269/2021 and Rede NanoSaúde - E-26/210.139/2019) for financial support.

Institutional Review Board Statement: Not applicable.

Informed Consent Statement: Not applicable.

Data Availability Statement: The data that support the findings of this study are available from the corresponding authors upon reasonable request.

Acknowledgments: The authors are grateful to the Multi-user Microscopy Nucleus of COPPE/Federal University of Rio de Janeiro (Rio de Janeiro, RJ, Brazil) for microscopy analysis. To Surface and Thin Film Laboratory (PEMM/COPPE/UFRJ) by the performance of FTIR and UV-Vis spectroscopy analysis, and to the Inorganic chemistry department from Chemistry Institute of Federal University of Rio de Janeiro (UFRJ), for the UV-Vis spectroscopy analysis on thin films.

Conflicts of Interest: The authors declare no conflict of interest.

References

1. Canbolat, M.F.; Celebioglu, A.; Uyar, T. Drug delivery system based on cyclodextrin-naproxen inclusion complex incorporated in electrospun polycaprolactone nanofibers. *Colloids Surf. B: Biointerfaces* **2014**, 115, 15-21. https://doi.org/10.1016/j.colsurfb.2013.11.021
2. Turan, C.U.; Guvenilir, Y. Electrospun poly(ω-pentadecalactone-*co*-ε-caprolactone)/gelatin/chitosan ternary nanofibers with antibacterial activity for treatment of skin infections. *Eur. J. Pharm. Sci.* **2022**, 170, 106113. https://doi.org/10.1016/j.ejps.2021.106113
3. De Oliveira, B.G.R.B.; Oliveira, B.C.; Deutsch, G.; Pessanha, F.S.; Thiré, R.M.S.M.; de Castilho, S.R. rhEGR-loaded hydrogel in the treatment of chronic wounds in patients with diabetes: Clinical cases. *Gels* **2022**, 8(8), 523. https://doi.org/10.3390/gels8080523
4. Yuan, Y.; Ding, L.; Chen, Y.; Chen, G.; Zhao, T.; Yu, Y. Nano-silver functionalized polysaccharides as platform for wound dressings: A review. *Int. J. Biolog. Macromol*. **2022**, 194, 644-653. https://doi.org/10.1016/j.ijbiomac.2021.11.108
5. Abrigo, M.; Mc Arthur, S.L.; Kinsgshott, P. Electrospun nanofibers as dressings for chronic wound care: Advances, Challenges and futures prospects. *Macromol. Biosci.* **2014**, 14, 772–792. https://doi.org/10.1002/mabi.201300561
6. Solovieva, E.V.; Teterina, A.Y.; Klein, O.I.; Komlev, V.S.; Alekseev, A.A. Panteleyev, A.A. Sodium alginate-based composites as a collagen substitute for skin bioengineering. *Biomed. Mater.* **2020**, 16, 015002. https://doi.org/10.1088/1748-605X/abb524
7. Serbezeanu, D.; Bargan, A.; Homocianu, M.; Aflori, M.; Rimbu, C.M.; Enache, A.A.; Vlad-Bubulac, T. Electrospun polyvinyl alcohol loaded with phytotherapeutic agents for wound healing applications. *Nanomaterials* **2021**, 11(12), 3336. https://doi.org/10.3390/nano11123336
8. Gangwar, A.; Kumar, P.; Singh, R.; Kush, P. Recent advances in mupirocin delivery strategies for the treatment of bacterial skin and soft tissue infection. *Future Pharmacology* **2021**, 1(1), 80-103. https://doi.org/10.3390/futurepharmacol1010007
9. Krysiak, Z.J.; Stachewicz, U. Electrospun fibers as carriers for topical drug delivery and release in skin bandages and patches for atopic dermatitis treatment. *WIREs Nanomed. Nanobiotechnol*. **2022**, e1829. https://doi.org/10.1002/wnan.1829
10. Unalan, I.; Slavik, B.; Buettner, A.; Goldmann, W.H.; Frank, G.; Boccaccinni, A.R. Physical and antibacterial properties of peppermint essential oil loaded poly(ε-caprolactone) (PCL) electrospun fiber mats for wound healing. *Front. Bioeng. Biotechnol*. **2019**, 26, 346. https://doi.org/10.3389/fbioe.2019.00346
11. Jawhari, F.Z.; Moussaori, A.E.; Bourhia, M.; Imtara, H.; Mechchate, H.; Es-Safi, I.; Ullah, R.; Ezzeldin, E.; Mostafa, G.A.; Grafov, A.; Ibenmoussa, S.; Bousta, E.; Bari, A. *Anacyclus pyrethrum* (L): chemical composition, analgesic, anti-inflammatory, and wound healing properties. *Molecules* **2020**, 25(22), 5469. https://doi.org/10.3390/molecules25225469
12. Shah, M.Z.; Guan, Z.H.; Din, A.U.; Ali, A.; Rehman, A.U.; Jan, K.; Faisal, S.; Saud, S.; Adnan, M.; Wahid, F.; Alamri, S.; Siddiqui, M.H.; Ali, S.; Nasim, W.; Hammad, H.M.; Fahad, S. Synthesis of silver nanoparticles using Plantago lanceolata extract and assessing their antibacterial and antioxidant activities. *Sci. Rep*. **2021**, 11, 20754. https://doi.org/10.1038/s41598-021-00296-5
13. Fernandes, D.M.; Barbosa, W.S.; Rangel, W.S.P.; Valle, I.M.M.; Matos, A.P.S.; Melgaço, F.G.; Dias, M.L.; Ricci Júnior, E.; da Silva, L.C.P.; de Breu, L.C.L.; Monteiro, M.S.S.B. Polymeric membrane based on polylactic acid and babassu oil for wound healing. *Mater. Today Commun*. **2021**, 26, 102173. https://doi.org/10.1016/j.mtcomm.2021.102173
14. Gorain, B.; Pandey, M.; Leng, N.H.; Yan, C.W.; Nie, K.W.; Kaur, S.J.; Marshall, V.; Sisinthy, S.P.; Panneerselvam, J.; Mologulu, N.; Kesharwani, P.; Choudhury, H. Advanced drug delivery systems containing herbal components for wound healing. *Int. J. Pharm*. **2022**, 617, 121617. https://doi.org/10.1016/j.ijpharm.2022.121617
15. Ouedrhiri, W.; Mechchate, H.; Moja, S.; Baudino, S.; Saleh, A.; Al-Kamaly, O.M.; Grafov, A.; Greche, H. Optimized antibacterial effects in a designed mixture of essential oils of Myrtus communis, Artemisa herba-alba and Thymus serpyllum for wide range of applications. *Foods* **2022**, 11(1), 132. https://doi.org/10.3390/foods11010132
16. Mancipe, J.M.A.; Dias, M.L.; Thiré, R.M.S.M. Type I collagen – Poly (vinyl alcohol) electrospun nanofibers: FTIR study of the collagen helical structure preservation. *Polym-Plast. Technol. Mater.* **2022**, 61(8), 846-860. http://doi.org./10.1080/25740881.2022.2029887
17. Raju, N.R.; Silina, E.; Stupin, V.; Manturova, N.; Chidambaram, S.B.; Achar, R.R. Multifunctional and smart wound dressing – A review on recent research advancements in skin regenerative medicine. *Pharmaceutics* **2022**, 14(8), 1574. https://doi.org/10.3390/pharmaceutics14081574
18. Toledo, A.L.M.M.; da Silva, T.N.; Vaucher, A.C.S.; Miranda, A.H.H.; Silva, G.C.C.; Vaz, M.E.R.; da Silva, L.V.; Barradas, T.N.; Picciani, P.H.S. Polymer nanofibers for biomedical applications: Advances in electrospinning. *Curr. Appl. Polym. Sci.* **2021**, 4(3), 190-209. http://doi.org/10.2174/2452271604666211122122557

19. Ghomi, E.R.; Khosravi, F.; Neisiany, R.E.; Shakiba, M.; Zare, M.; Lakshminarayanan, R.; Chellappan, V.; Adbouss, M.; Ramakrishna, S. Advances in electrospinning of aligned nanofiber scaffolds used for wound dressings. *Curr. Opin. Biomed. Eng*. **2022**, 22, 100393. https://doi.org/10.1016/j.cobme.2022.100393
20. Keler, K.; Daglilar, S.; Gunduz. O.; Yuksek, M.; Sahin, Y.M.; Ekren, N.; Oktar, F.N.; Salman, S. Mechanical behavior of PCL nanofibers. *Key Eng. Mater*. **2016**, 696, 196-201. https://doi.org/10.4028/www.scientific.net/KEM.696.196
21. Altun, E.; Ahmed, J.; Aydogdu, M.O.; Harker, A.; Edirisinghe, M. The effect of solvent and pressure on polycaprolactone solutions for particle and fibre formation. *Eur. Polym. J.* **2022**, 173, 111300. https://doi.org/10.1016/j.eurpolymj.2022.111300
22. Zubair, M.; Ekholm, A.; Nybom, H.; Renvert, S.; Widen, C.; Rumpunen, K. Effects of Plantago major L. leaf extracts on oral epithelial cells in a scratch assay. *J. Ethnopharmacol* **2012**, 1412(3), 825-830. https://doi.org/10.1016/j.jep.2012.03.016
23. Samuelsen, A.B. The traditional uses, chemical constituents and biological activities of Plantago major L. A review. *J. Ethnopharmacol.* **2000**, 71(1-2), 1-21. https://doi.org/10.1016/S0378-8741(00)00212-9
24. Farid, A.; Sheibani, M.; Shojaii, A.; Noori, M.; Motevalian, M. Evaluation of anti-inflammatory effects of leaf and seed extracts of *Plantago major* on acetic acid-induced ulcerative colitis in rats. *J. Ethnopharmacol.* **2022**, 298, 115595. https://doi.org/10.1016/j.jep.2022.115595
25. Soliman, M.A.; Galal, T.M.; Naim, M.A.; Khalafallah, A.A. Seasonal variation in the secondary metabolites and antimicrobial activity of *Plantago major L.* from Egyptian heterogenic habitats. Egyptian *J. Bot.* **2022**, 62, 255-273. https://doi.org/10.21608/ejbo.2021.94145.1778
26. Nikaeen, G.; Rahmdell, S.; Samari, F.; Mahdavinia, S. Central composite design for optimizing the biosynthesis of silver nanoparticles using Plantago major extract and investigation antibacterial, antifungal and antioxidant activity. *Sci. Rep*. **2020**, 10, 9642. https://doi.org/10.1038/s41598-020-66357-3
27. Lukova, P.; Nikolova, M.; Petit, E.; Elboutachfaiti, R.; Vasileva, T.; Katsarov, P.; Manev, H.; Gardarin, C.; Pierre, G.; Michaud, P.; Iliev, I.; Delattre, C. Prebiotic activity of poly- and oligosaccharides from *Plantago major L.* leaves. *Appl. Sci.* **2020**, 10(8), 2648. https://doi.org/10.3390/app10082648
28. Gunathilake, K.D.P.P.; Ranaweera, K.K.D.S.; Rupasinghe, H.P.V. Invitro anti-inflammatory properties of selected green leafy vegetables. *Biomedicines* **2018**, 6(4), 107. https://doi.org/10.3390/biomedicines6040107
29. Silva Neto, A.R.; Sousa, A.C.S.O.; Camboim, L.F.R.; da Silva, J.P.R.; Maia Filho, A.L.M.; Leal, F.R.; Costa, C.A.C.B.; Freitas, J.M.D.; de Freitas, J.D.; Marques, R.B.; Uchôa, V.T. Phytochemical profile and analgesic Activity of the extract from *Plantago Major L. Rev. Virtual Quim.* **2023**, 1-11. http://doi.org/10.21577/1984-6835.20220104
30. Keshavari, A.; Montaseri, H.; Akrami, R.; Saravestani, H. M.; Khosravi, F.; Foolad, S.; Zardosht, M.; Zareie, S.; Saharkhiz, M. J.; Shahriarirad, R. Therapeutuc efficacy of great plantain (Plantago major L.) in the treatment of second-degree burn wounds: A case-control study. *Int. J. Clin. Pract*. **2022**, 2022, 4923277 https://doi.org/10.1155/2022/4923277
31. Ghanadian, M.; Soltani, R.; Homayouni, A.; Khorvash, F.; Jouabadi, S. M.; Abdollahzadeh, M. The effect of Plantago major hydroalcoholic extract on the healing of diabetic foot and pressure ulcers: A randomized open-label controlled clinical trial. *Int. J. Low. Extrem. Wounds* **2022**, 2022, 1-7. https://doi.org/10.1177/15347346211070723
32. Amini, M.; Kherad, M.; Mehrabani, D.; Azarpira, N.; Panjehshahin, M.R.; Tanideh, N. Effect of Plantago major on burn wound healing in rat. *J. Appl. Anim. Res*. **2010**, 37, 53-56. https://doi.org/10.1080/09712119.2010.9707093
33. Reina, E.; Al-Shibani, N.; Allam, E.; Gregson, K.S.; Kowolik, M.; Windson, J. The effects of Plantago major on the activation of the neutrophil respiratory burst. *J. Tradit. Complement. Med.* **2013**, 3(4), 268–272. https://doi.org/10.4103/2225-4110.119706
34. Golkar, P.; Kalani, S.; Allafchian, A.R.; Mohammadi, H.; Jalali, S.A.H. Fabrication and characterization of electrospun Plantago major seed mucilage/PVA nanofibers. *J. Appl. Polym. Sci*. **2019**, 136(32), 47852. https://doi.org/10.1002/app.47852
35. De Castro, K.C.; Silva, E.K.; Campos, M.G.N.; Mei, L.H.I. Hyaluronic acid/polyvinyl alcohol electrospun nanofiber membranes loaded with Plantago major extract for smart wound dressings. *ACS Appl. Nano Mater*. **2022**, 5(9), 12616-12625. https://doi.org/10.1021/acsanm.2c02402
36. Mello, J.C.; Gonzalez, M.V.D.; Moraes, V.W.R.; Prieto, T.; Nascimento, O.R.; Rodrigues, T. Protective effect of Plantago major extract against t-BOOH-Induced mitochondrial oxidative damage and cytotoxicity. *Molecules* **2015**, 20(10), 17747-17759. https://doi.org/10.3390/molecules201017747
37. Mancipe, J.M.A.; Dias, M.L.; Thiré, R.M.S.M. Morphological evaluation of electrospun polycaprolactone fibers depending on the type of solvent. *Matéria (Rio J)* **2019**, 24(3). e-12400. https://doi.org/10.1590/s1517-707620190003.0713
38. Rabello, L.G.; Ribeiro, R.C.C. Bio-based polyurethane resin: An ecological binder for a novel class of building materials-composites. *Mater. Lett*. **2022**, 311, 131566. https://doi.org/10.1016/j.matlet.2021.131566

39. Mouro, C.; Gomes, A.P.; Ahonen, M.; Fangueiro, R.; Gouveia, I.C. Chelidonium majus L. incorporated emulsion electrospun PCL/PVA_PEC nanofibrous meshes for antibacterial wound dressing applications. *Nanomaterials* **2021**, 11, 1785. https://doi.org/10.3390/nano11071785
40. Souza, J.P.L.M.; Pires, L.O.; dos Santos, R.F.; Prudêncio, E.R.; Sant'Ana, L.D.; Ferreira, D.A.S.; Castro, R.N. Estudo químico e potencial antimicrobiano da própolis brasileira produzida por diferentes espécies de abelhas. *Rev. Virtual Quim*. **2019**, 11(5), 1480-1497. http://doi.org/10.21577/1984-6835.20190103
41. Salgueiro, F.B.; Castro, R.N. Comparação entre a composição química e capacidade antioxidante de diferentes extratos de própolis verde. *Quim. Nova* **2016**, 39(10), 1192-1199. http://doi.org/10.21577/0100-4042.20160136
42. Anaya-Mancipe, J.M.; Pereira, L.C.B.; Borchio, P.G.M.; Dias, M.L.; Thiré, R.M.S.M. Novel polycaprolactone (PCL)-type I collagen core-shell electrospun nanofibers for wound healing applications. *J. Biomed. Mater. Res. B Appl. Biomater.* **2022**, 1-16. http://doi.org/10.1002/jbm.b.35156
43. Snetkov, P.; Rogacheva, E.; Kremleva, A.; Morozkina, S.; Uspenskaya, M.; Kraeva, L. In-Vitro antibacterial activity of curcumin-loaded nanofibers based on hyaluronic acid against multidrug-resistant ESKAPE pathogens. *Pharmaceutics* **2022**, 14(6), 1186. https://doi.org/10.3390/pharmaceutics14061186
44. Calatayud, M.; López-de-Dicastillo, C.; López-Carballo, G.; Vélez, D.; Muñoz, P.H.; Gavara, R. Active films based on cocoa extract with antioxidant, antimicrobial and biological applications. *Food Chem.* **2013**, 139(1-4), 51-58. https://doi.org/10.1016/j.foodchem.2013.01.097
45. CLASI. Methods for Dilution Antimicrobial Susceptibility Tests for Bacteria That Grow Aerobically, Approved Standard – Ninth edition, document M07-A9, Clinical and Laboratory Standards Institute, Wayne, PA, 2012.
46. Anusree, S. S., Nisha, V. M., Priyanka, A., Raghu, K. G. Insulin resistance by TNF-α is associated with mitochondrial dysfunction in 3T3-L1 adipocytes and is ameliorated by punicic acid, a PPARγ agonist, Mol Cell Endocrinol 2015, 413, 120–128. https://doi.org/10.1016/J.MCE.2015.06.018
47. Chookalaii, H.; Riahi, H.; Shariatmadari, Z.; Mazarei, Z.; Hashtroudi, M.S. Enhancement of total flavonoid and phenolic contents in Plantago major L. with growth promoting cyanobacteria. *J. Agr. Sci. Tech.* **2020**, 22(2), 505-518. http://jast.modares.ac.ir/article-23-21403-en.html
48. Karima, S.; Farida, S.; Mihoub, Z.M. Antioxidant and antimicrobial activities of Plantago major. *Int. Pharm. Pharm Sci.* **2015**, 5(7), 58-64.
49. Süntar I.; Akkol, K. E.; Nahar, L.; Sarker, S. D. Wound healing and antioxidant properties do they coexist in plants?. *Free Radic. Antioxid*. **2012**, 2(2), 1-7. https://doi.org/10.5530/ax.2012.2.2.1
50. Ghanadian, M.; Soltani, R.; Homayouni, A.; Khorvash, F.; Jouabadi, S.M.; Abdollahzadeh, M. The effect of Plantago major hydroalcoholic extract on the healing of diabetic foot and pressure ulcers: A randomized open-label controlled clinical trial. *Int. J. Low. Extrem. Wounds* **2022**, 2022, 1-7. https://doi.org/10.1177/153473462110707
51. Adom, M.B.; Taher, M.; Mutalabisin, M.F.; Amri, M.S.; Kudos, M.B.A.; Sulaiman, M.W.A.W.; Sengupta, P.; Susanti, D. Chemical constituents and medical benefits of Plantago major. *Biomed. Pharmacother*. **2017**, 96, 348-360. https://doi.org/10.1016/j.biopha.2017.09.152
52. Murray, C. J.; Ikuta, K. S.; Sharara, F.; Swetschinski, L.; Aguilar, G. R.; Gray, A.; Naghavi, M.; Global burden of bacterial antimicrobial resistance in 2019: a systematic analysis. *The Lancet* 2022;399(10325):629-655.
53. Carlos, A.L.M.; Mancipe, J.M.A.; Dias, M.L.; Thiré, R.M.S.M. Poly(3-hydroxybutyrate-co-3-hydroxyvalerate) core-shell spun fibers produced by solution blow spinning for bioactive agent's encapsulation. *J. Appl. Polym. Scie.* **2022**, 139(18), 52081. https://doi.org/10.1002/app.52081
54. Figueiredo, A.C.; Anaya-Mancipe, J.M.; de Barros, A.O.S.; Santos-Oliveira, R.; Dias, M.L.; Thiré, R.M.S.M. Nanostructured electrospun polycaprolactone – propolis mats composed of different morphologies for potential use in wound healing. *Molecules* **2022**, 27(16), 5351. https://doi.org/10.3390/molecules27165351
55. Czarnecka, K.; Wojasinski, M.; Ciach, T.; Sajkiewicz, P. Solution blow spinning of polycaprolactone – rheological determination of spinning and effect of processing conditions on fiber diameter and alignment. *Materials* **2021**, 14, 1463. https://doi.org/10.3390/ma14061463
56. Oviedo, M.; Montoya, Y.; Agudelo, W.; García-García, A.; Bustamante, J. Effect of molecular weight and nanoarchitecture of chitosan and polycaprolactone electrospun membranes on physicochemical and hemocompatible properties for wound dressing. *Polymers* **2021**, 13(24), 4320. https://doi.org/10.3390/polym13244320
57. Kulkarni, D., Musale, S., Panzade, P., Paiva-Santos, A.C., Sonwane, P., Madine, M., Choundhe, P., Giram, P., Cavalu, S. Surface functionalization of nanofibers: the multifaceted approach for advanced biomedical applications. *Nanomaterials* **2022**, 12(21), 3899. https://doi.org/10.3390/nano12213899
58. Toledo, A.L.M.M.; Ramalho, B.S.; Picciani, L.S.; Baptista, L.S.; Martinez, A.M.B.; Dias, M.L. Effect of three different amines on the surface properties of electrospun polycaprolactone mats. *Int. J. Polym. Mater. Polym. Biomater.* **2021**, 70(17), 1258-1270. https://doi.org/10.1080/00914037.2020.1785463

59. Elzein, T.; Nasser-Eddine, M.; Delaite, C.; Bistac, S.; Dumas, P. FTIR study of polycaprolactone chain organization at interfaces. *J. Colloid Interface Sci.* **2004**, 273(2), 381-387. https://doi.org/10.1016/j.jcis.2004.02.001
60. Oliveira, R.N.; Mancini, M.C.; de Oliveira, F.C.S.; Passos, T.M.; Quilty, B, Thiré, R.M.S.M.; McGuinness, G.B. FTIR analysis and quantification of phenols and flavonoids of five commercially available plant extracts used in wound healing. *Matéria (Rio J)* **2016**, 21(3), 11743. https://doi.org/10.1590/S1517-707620160003.0072
61. Dewi, A.F.; Prajitno, A.; Yuniarti, A. Phytochemicals and the ability of Plantago major Linn. extract to inhibit the growth of Aeromonas hydrophila. *J. Exp. Life Sci.* **2019**, 9(2), 70-75. https://doi.org/10.21776/ub.jels.2019.009.02.02
62. Behbahani, B.A.; Yazdi, F.T.; Shahidi, F.; Hesarinejad, M.A.; Mortazavi, S.A.; Mohebbi, M. *Plantago major* seed mucilage: Optimization of extract and some physicochemical and rheological aspects. *Carbohydr. Polym.* **2017**, 155, 68-77. https://doi.org/10.1016/j.carbpol.2016.08.051
63. Sukweenadhi, J.; Setiawan, K.I.; Avanti, C.; Kartini, K.; Rupa, E.J.; Yang, D.C. Scale-up of green synthesis and characterization of silver nanoparticles using ethanol extract of *Plantago Major L.* leaf and its antibacterial potential. *S. Afr. J. Chem. Eng.* **2021**, 38, 1-8. https://doi.org/10.1016/j.sajce.2021.06.008
64. Mohammed, N.K. Phytochemical screening by FTIR spectroscopy analysis and anti-bacterial activity of methanolic extract of selected medicinal plant of Anethum graveolens and Plantago major. *Ann. Romanian Soc. Cell Biol.* **2021**, 25(4), 3110-3122. https://www.annalsofrscb.ro/index.php/journal/article/view/2852
65. Bikiaris, N.D.; Koumentakou, I.; Michailidou, G.; Kostoglou, M.; Vlachou, M.; Barmpalexis, P.; Karavas, E. Papageorgiou, G.Z. Investigation of molecular weight, polymer concentration and process parameters factors on the sustained release of the anti-multiple-sclerosis agent teriflunomide from poly(ε-caprolactone) electrospun nanofibrous matrices. *Pharmaceutics* **2022**, 14(8), 1693. https://doi.org/10.3390/pharmaceutics14081693
66. Wang, X.; Zhao, H.; Turng, L.S.; Li, Q. Crystalline morphology of electrospun poly(ε-caprolactone) (PCL) nanofibers. *Ind. Eng. Chem. Res.* **2013**, 52(13), 4939-4949. https://doi.org/10.1021/ie302185e
67. Krysiak, Z.J.; Stachewicz, U. Urea-based patches with controlled release for potential atopic dermatitis treatment. *Pharmaceutics* **2022**, 14(7), 1494. https://doi.org/10.3390/pharmaceutics14071494
68. Pedrosa, M.C.G.; dos Anjos, S.A.; Mavropoulos, E.; Bernardo, P.L.; Granjeiro, J.M.; Rossi, A.M.; Dias, M.L. Structural and biological compatibility of polycaprolactone/zinc-hydroxyapatite electrospun nanofibers for tissue regeneration. *J. Bioact. Compat. Polym.* **2021**, 36(4), 314-333. https://doi.org/10.1177/08839115211022448
69. Saraiva, M.M.; Campelo, M.S.; Câmara-Neto, J.F.; Lima, A.B.N.; Silva, G.A.; Dias, A.T.F.F.; Ricardo, N.M.P.S.; Kaplan, D.L.; Ribeiro, M.E.N.P. Alginate/polyvinyl alcohol films for wound healing: Advantages and challenges. *J. Biomed. Mater. Res. B* **2022**, 351465. https://doi.org/10.1002/jbm.b.35146
70. Karizmenh, M.S.; Poursamar, S.A.; Kefayat, A.; Farahbakhsh, Z.; Rafienia, M. An in vitro and in vivo study of PCL/chitosan electrospun mat on polyurethane/propolis foam as a bilayer wound dressing. *Biomaterials Advances* **2022**, 135, 112667. https://doi.org/10.1016/j.msec.2022.112667
71. Dias, J.R.; Sousa, A.; Augusto, A.; Bártolo, P.J.; Granja, P.L. Electrospun polycaprolactone (PCL) degradation: Na in vitro and in vivo study. *Polymers* **2022**, 14(160, 3397. https://doi.org/10.3390/polym14163397
72. Zhang, X.; Yang, L.; Zhang, C.; Danhua, L.; Meng, S.; Zhang, W.; Meng, S. Effect on polymer permeability and solvent removal rate on in situ forming implants: Drug burst release and microstructure. *Pharmaceutics* **2019**, 11(10), 520. https://doi.org/10.3390/pharmaceutics11100520
73. Shirley, K.P.; Windsor, J.; Eckert, G.J.; Gregory, R.L. In vitro effects of Plantago major extract, Aucubin, and Baicalein on candida albicans biofilm formation, metabolic activity, and cell surface hydrophobicity. *J. Prosthodontic.* **2017**, 26, 508-515. https://doi.org/10.1111/jopr.12411
74. Araújo, J.; Dobrovolski, M.; Kozlowski-Júnior, V.A.; Rezende, M. Use of Plantago major for the control of dental biofilm: Case report. *Res. Soc. Dev.* **2021**, 10, e29610111491. http://doi.org/10.33448/rsd-v10i1.1191
75. Alizadeh, B.B.; Shahidi, F.; Tabatabaei, Y.F., Mortazavi, S.A.; Mohebbi, M. The antimicrobial effect and interaction between the aqueous and ethanolic extract of Plantago major on Staphylococcus aureus, Listeria innocua, Escherichia coli and Pseudomonas aeruginosa In vitro. *Iran. J. Infect Dis. Trop. Med.* **2017**, 21(75), 1-8.
76. Trinidade, G.O.; Alves, V.H.; Mariño, P.A.; Maldaner, G.; Menezes, A.P.S.; dos Reis, R.O. Triagem fitoquímica e avaliação do potencial antibacteriano de extratos das folhas de Plantago major L. *Rev. Iniciação Cientifica Universidade Vale do Rio Verde* **2018**, 9(1), 41-48.

77. Petrović, M.; Jovanović, M.; Lević, S.; Nedović, V.; Mitić-Ćulafić, D.; Semren, T.Ž.; Veljović, S. Valorization potential of Plantago major L. solid waste remaining after industrial tincture production: Insight into the chemical composition and bioactive properties. *Waste and Biomass Valorization* **2022**, 13, 1639-1651. https://doi.org/10.1007/s12649-021-01608-6
78. Razik, B.M.A.; Hasan, H.A.; Murtadha, M.K.; The study of antibacterial activity of Plantago major and Ceratonia siliqua. *Iraqi Postgrad Med. J.* **2012**, 11, 130-135.